Electronic Supplementary Material (ESI) for Dalton Transactions.

Supporting Information

Triazine covalent organic framework (COF)/θ-Al_2O_3 composites for supercapacitors application

Lei Liu, Di Cui, Shuran Zhang, Wei Xie*, Chan Yao, Na Xu, and Yanhong Xu*

Key Laboratory of Preparation and Applications of Environmental Friendly Materials (Jilin Normal University), Ministry of Education, Changchun, 130103, Jilin, PR China.

** Corresponding author*

E-mail: xiew1415@163.com; xuyh198@163.com

Contents

Section A. Materials and instruments

2,4,6-tris(4-aminophenyl)-1,3,5-triazine was purchased from Alfa, 2,5-dihydroxyterephthalaldehyde was purchased from Sanbang Chemical. Used all solvents were purchased from Aladdin.

Fourier transform Infrared (FT-IR) spectra were recorded on a Perkin-elmer model FT-IR-frontier infrared spectrometer. For all FT-IR tests, a small amount of sample can be directly mixed with potassium bromide and ground into a powder, and then compressed, and the pressed product can be directly tested. The solid-state UV-visible analyzer was used for Jasco V-770 spectrometer. Solid-state ^{13}C CP/MAS NMR measurements were recorded using a Bruker AVANCE III 400 WB spectrometer at a MAS rate of 5 kHz and a CP contact time of 2 ms. X-ray photoelectron spectra (XPS) were recorded on an ESCALAB250Xi electron spectrometer (Thermo Fisher Scientific Inc., Waltham, MA, USA). Field-emission scanning electron microscopy (FE-SEM) images were performed on a JEOL model JSM-6700 operating at an accelerating voltage of 5.0 kV. Powder X-ray diffraction (PXRD) data were recorded on a Rigaku model RINT Ultima III diffractometer by depositing powder on glass substrate, from $2\theta = 2.5°$ up to 40° with 0.02° increment. TGA analysis was carried out using a Q5000IR analyzer (TA Instruments) with an automated vertical overhead thermobalance. Before measurement, the samples were heated at a rate of 5 °C min^{-1} under nitrogen atmosphere. Nitrogen sorption isotherms were measured at 77 K with ASIQ (iQ-2) volumetric adsorption analyzer. Before measurement, the samples were degassed in vacuum at 120 °C for more than 10 h. The Brunauer-Emmett-Teller (BET) method was utilized to calculate the specific surface areas and pore volume. The non-local density functional theory (NLDFT) method was applied for the estimation of pore size and pore size distribution.

Electrochemical measurement was carried out in a standard three electrode system with a 1 M H_2SO_4 aqueous solution at 25 °C in a CHI 760 Eelectrochemical work station (CH instrument, USA). Active material (100 μg) coated carbon cloth, Pt wire and a saturated calomel electrodes were considered as working, counter and reference electrodes, respectively. The cyclic voltammograms (CVs) were recorded within a potential window of 0 V to 1 V in the scan rate range of 20 to 100 mV s^{-1}. Galvanostatic charge discharge (GCD) activity of electrode material was studied with different constant current density in a potential window of 0 V to 1 V. The electrochemical impedance spectra (EIS) were recorded by applying a sinusoidal perturbation of 5 mV in a frequency domain 0.01 to 10000 Hz.

Calculations of specific capacitance

Based on the GCD data, the gravimetric specific capacitance (Cm, F g^{-1}) was calculated using the following equation:

$$C\mathrm{m} = \frac{\mathrm{I} \times \mathrm{t}}{\mathrm{m} \times \Delta V}$$

where I is the discharge current (A), t is the discharge time (s), m is the mass of the active material (g), and ΔV is the potential change during the discharge process (V).

Section B. Synthetic procedures

Synthesis of θ-Al_2O_3

Weigh nano-Al_2O_3 (8.5 g) and put it into corundum container, then the container was placed in tube furnace, heated at 1200 °C for 2 h under the nitrogen atmospheres. After cooling to room temperature, θ-Al_2O_3 was obtained as a white solid powder (yield: 27%).

Synthesis of θ-Al_2O_3-NH_2

Firstly, θ-Al_2O_3 (2 g, 19.62 mmol) was added to the flask, and then hydrochloric acid solution was added to the flask. The activated θ-Al_2O_3 powder was obtained by gently stirring and soaking for 5 h, and then filtering, washing the filter cake with water for three times, freeze drying. Then, APTES (0.9829 g, 0.444 mmol) and activated θ-Al_2O_3 (0.4612 g, 4.52 mmol) were weighed and placed in the flask, and anhydrous toluene was used as the solvent and heated at 100 °C for 3 h under the nitrogen atmospheres. After cooling to room temperature, the obtained solid was filtered and washed with methanol, water and acetone for three times respectively, to get θ-Al_2O_3-NH_2 (yield: 79%).

Synthesis of θ-Al_2O_3-CHO

θ-Al_2O_3-NH_2 (0.015 g) and 1,3,5-benzenetricarboxaldehyde (0.015 g, 0.0925 mmol) were weighed and placed in polytetrafluoroethylene reactor, followed by 1,4-dioxane (15 mL) was added, and then the mixture was heated at 150 °C for 1 h in a constant temperature oven. After cooling to room temperature, the obtained solid was washed with methanol, water, and acetone for 3 times, respectively, to get θ-Al_2O_3-CHO (yield: 83%).

Synthesis of Al_2O_3@DHTA-COFs

A Pyrex tube was charged with θ-Al_2O_3-CHO (2 mg, or 10 mg, or 15 mg), 2,4,6-tris(4-aminophenyl)-1,3,5-triazine (40 mg, 0.112 mmol), and 2,5-dihydroxyterephthalaldehyde (20 mg, 0.145 mmol) in a mixed solution of 1,2-dichlorobenzene (1.6 mL), ethanol (0.5 mL), and acetic acid (6 M, 0.2 mL). The tube was frozen and vacuumed at 77 K (liquid nitrogen bath), and then sealed with flame. The mixture was heated at 120 °C for 72 h to afford a red precipitate, which was isolated by filtration, washed with anhydrous acetone for 5 times, and vacuum drying at 85 °C to afford 20%Al_2O_3@DHTA-COF, 50%Al_2O_3@DHTA-COF and 75%Al_2O_3@DHTA-COF, red powders with 82-87% isolated yield.

Preparation of DHTA-COF, θ-Al_2O_3-CHO and Al_2O_3@DHTA-COFs electrode materials

The electrode composed of DHTA-COF, θ-Al_2O_3-CHO and Al_2O_3@DHTA-COFs were fabricated by mixing the particular DHTA-COF, θ-Al_2O_3-CHO or Al_2O_3@DHTA-COFs (80%), Super-P carbon (10%) and polyvinylidene fluoride (PVDF) (10 % in N-methyl-2-pyrrolidone) as binder. Spread evenly on carbon cloth and dry at 60 ℃ for 12 h. The typical area and weights of electrode materials are 0.5×0.5 cm^2 and 0.1 mg, respectively.

Section C. Powder X-ray diffraction patterns

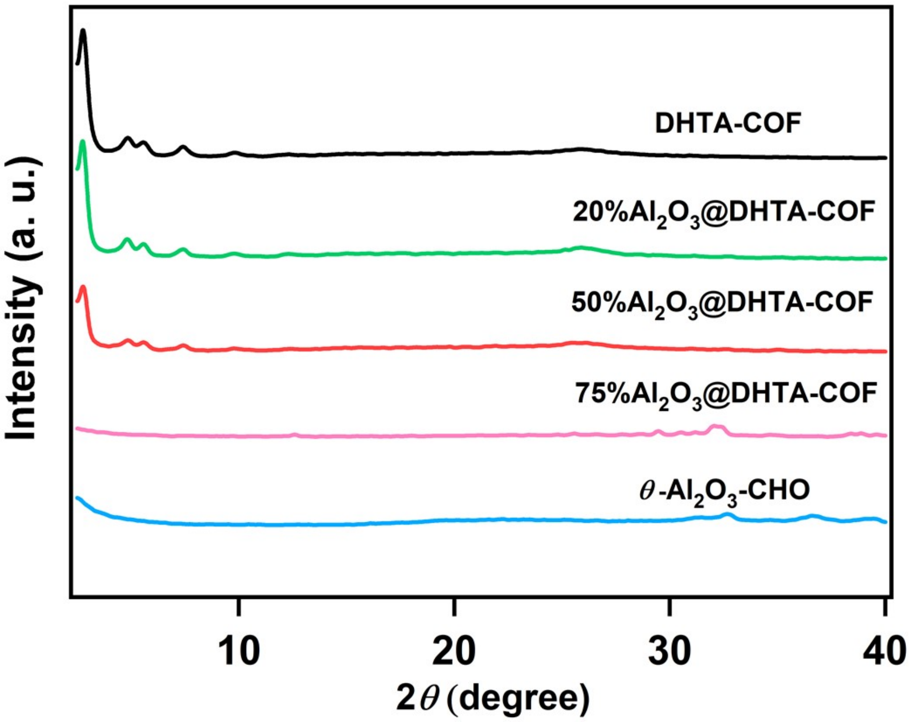

Fig. S1 Powder X-ray diffraction profiles of DHTA-COF, θ-Al_2O_3-CHO, and Al_2O_3@DHTA-COFs.

Section D. The solid-UV spectra

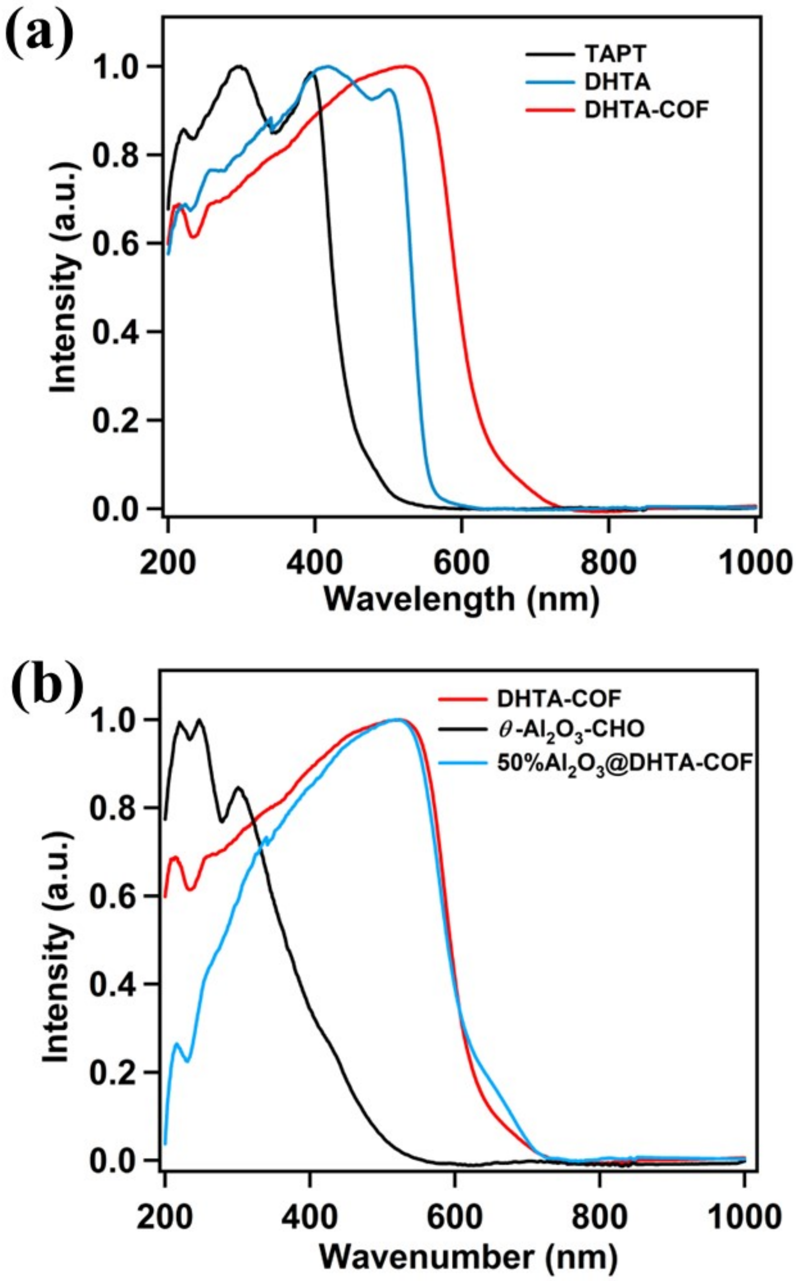

Fig. S2 Solid state UV spectra of (a) DHTA, TAPT, and DHTA-COF, (b) DHTA-COF, θ-Al_2O_3-CHO, and 50%Al_2O_3@DHTA-COF.

Section E. Stability

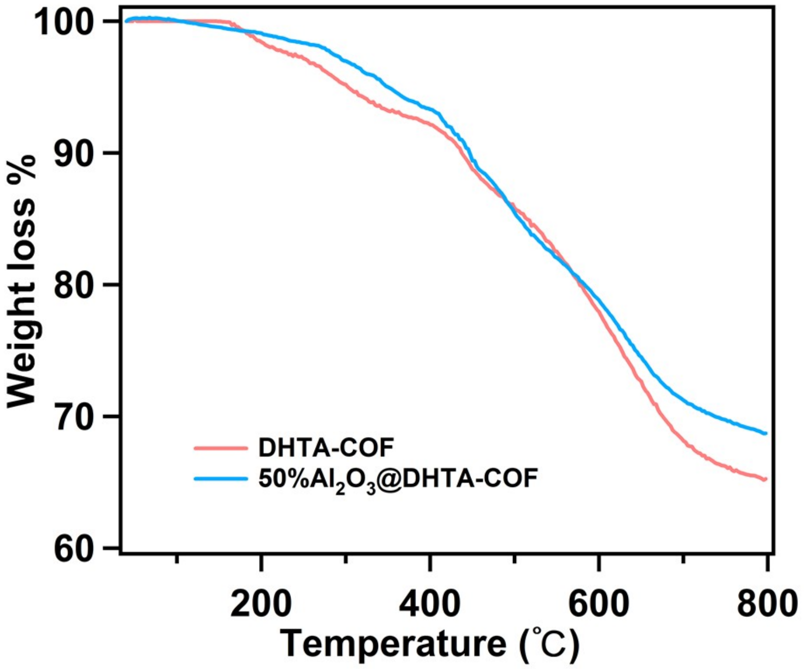

Fig. S3 TGA curves of DHTA-COF, 50%Al_2O_3@DHTA-COF.

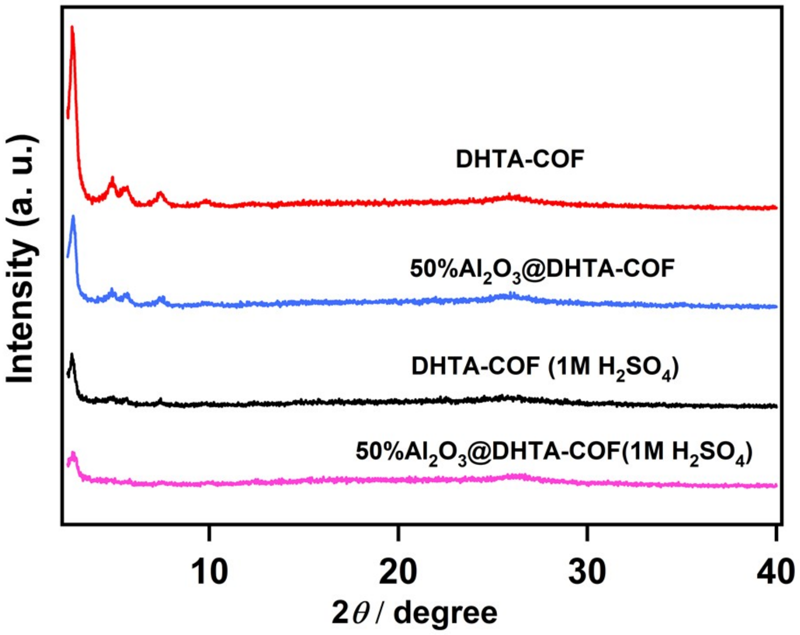

Fig. S4 PXRD patterns of the DHTA-COF and 50%Al_2O_3@DHTA-COF before and after soaked in 1.0 M H_2SO_4.

Section F. SEM images

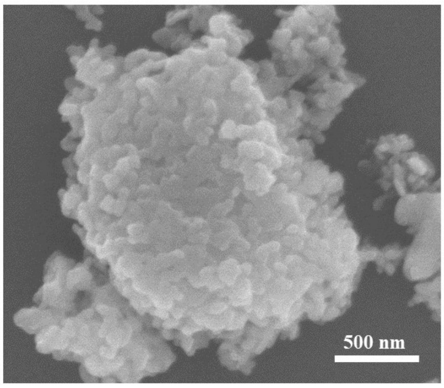

Fig. S5 The SEM picture of θ-Al_2O_3-CHO.

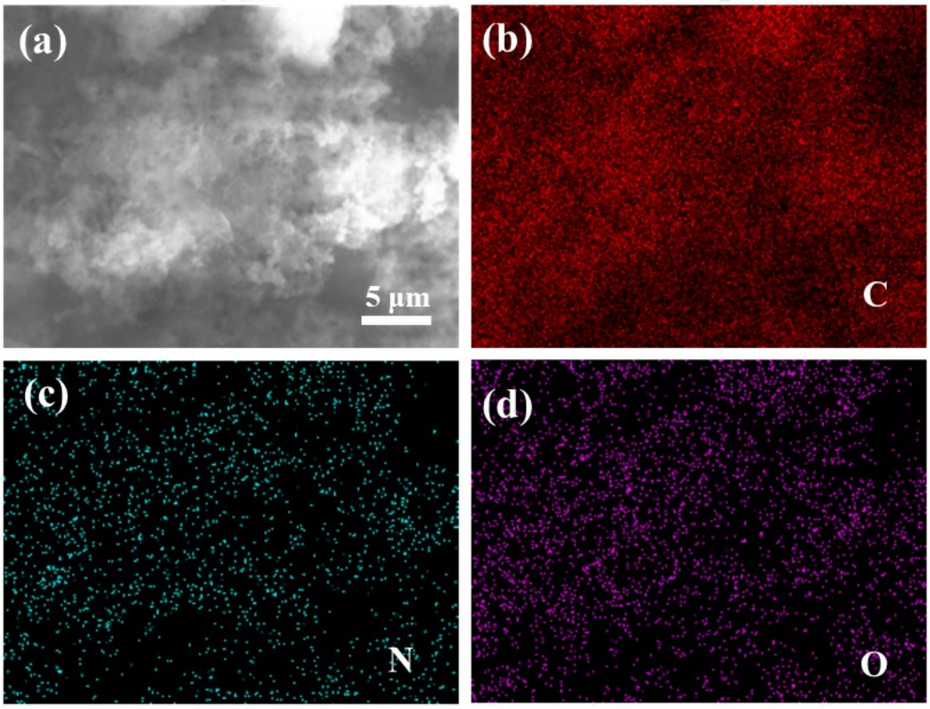

Fig. S6 (a) The corresponding elemental mapping images of (b) carbon, (c) nitrogen, and (d) oxygen in DHTA-COF.

Section G. N_2 adsorption isotherms

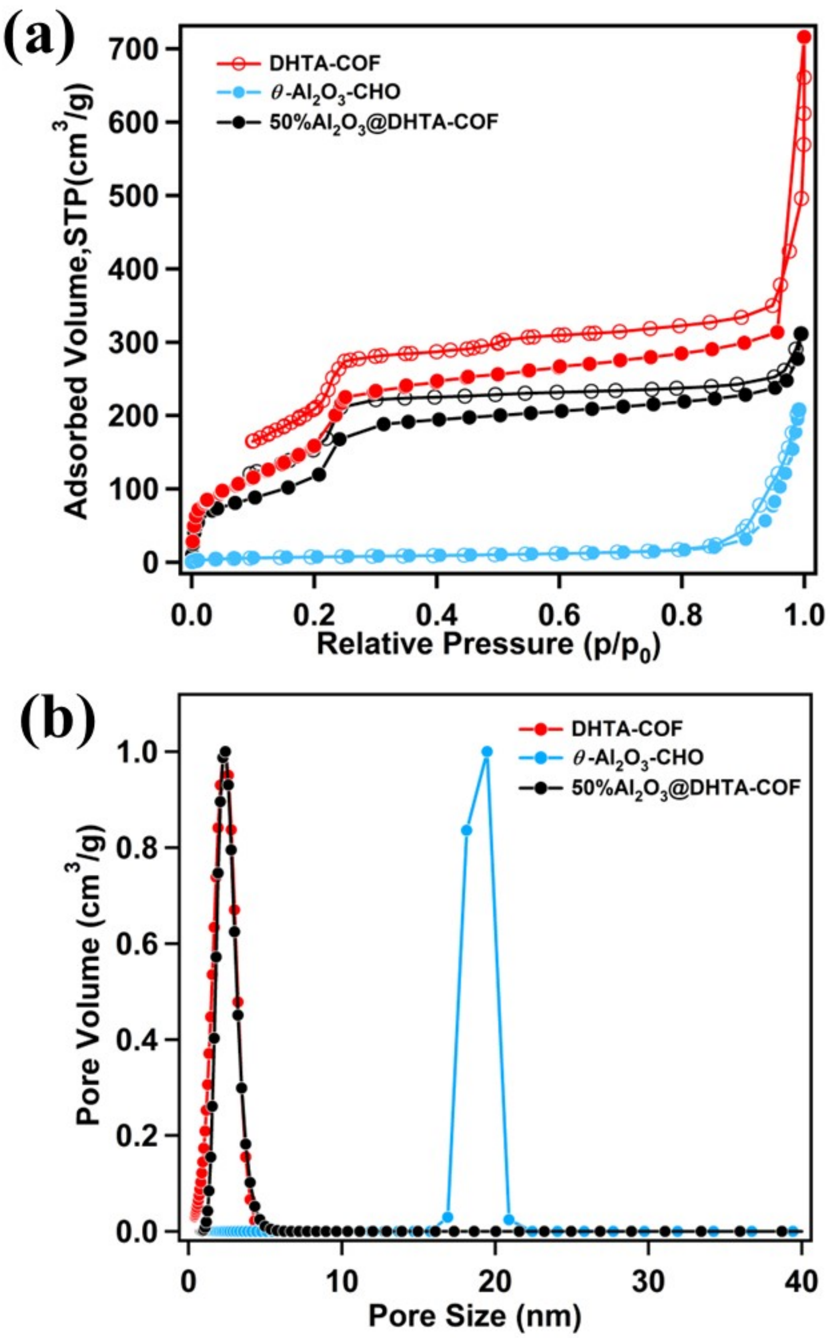

Fig. S7 (a) N_2 adsorption isotherms and (b) pore size distributions of DHTA-COF, θ-Al_2O_3-CHO, 50%Al_2O_3@DHTA-COF at 77 K.

Section H. Electrochemical study

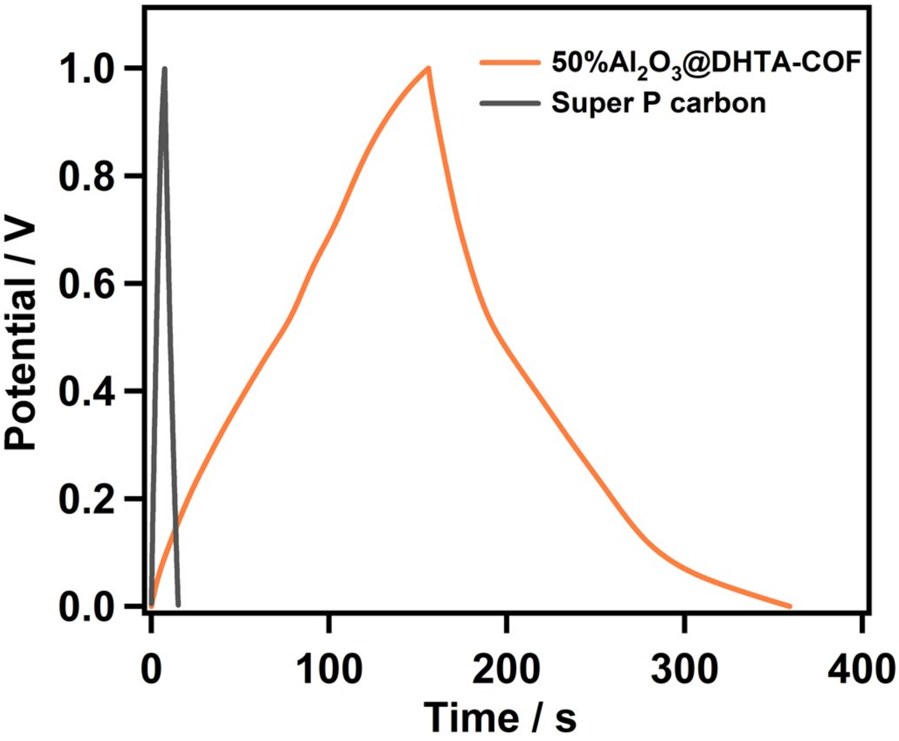

Fig. S8 GCD curves of the 50%Al_2O_3@DHTA-COF and Super P carbon.

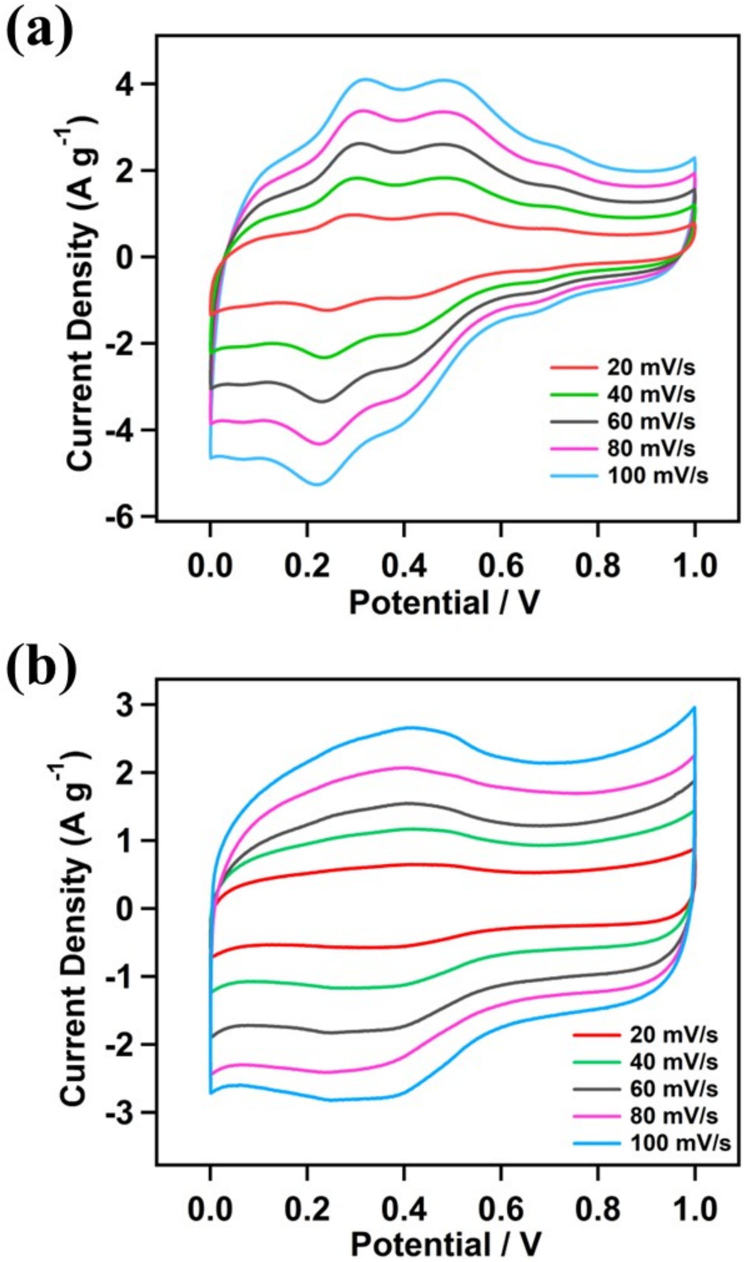

Fig. S9 CV curves of the (a) DHTA-COF, and (b) θ-Al_2O_3-CHO.

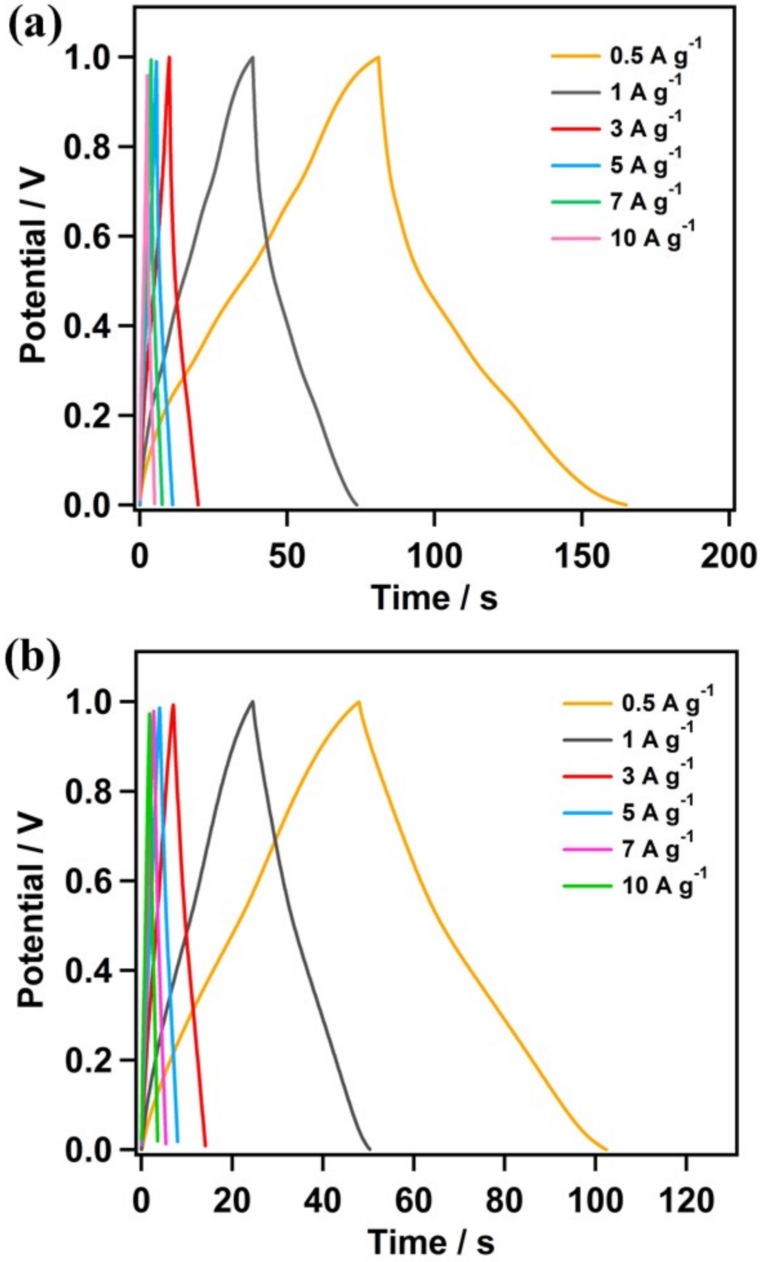

Fig. S10 GCD curves of the (a) DHTA-COF, and (b) θ-Al_2O_3-CHO.

Section I. Comparison of specific capacitance of 50%Al_2O_3@DHTA-COF with reported COF-based supercapacitors in literature

Table S1. Comparison of 50%Al_2O_3@DHTA-COF with some reported COF-based supercapacitors.

Polymers	***Specific capacitance*** **(F g^{-1})**	***Current density***	***Electrolyte***	**Refs.**
50%Al_2O_3@DHTA-COF	261.5	0.5 A g^{-1}	1 M H_2SO_4	This work
TpOMe-DAQ	135	0.35 A g^{-1}	3 M H_2SO_4	S1
Dq1Da1Tp	111	1.56 mA cm^{-2}	1 M H_2SO_4	S2
BFTB-PyTA	71	1 A g^{-1}	1 M KOH	S3
TPA-COFs	263.1	0.1 A g^{-1}	1 M H_2SO_4	S4
TaPa-Py COF	209	0.5 A g^{-1}	1 M H_2SO_4	S5
Phos-COF-1	100	1 A g^{-1}	3 M Na_2SO_4	S6
MWCNT@$COF_{TTA\text{–}DHTA}$	92.4	0.4 A g^{-1}	1 M Na_2SO_4	S7
C/rGO	234	0.8 A g^{-1}	6 M KOH	S8
COF	211	1 A g^{-1}	6 M KOH	S9
TDFP-1	418	0.5 A g^{-1}	0.1 M H_2SO_4	S10
TFP-NDA-COF	348	0.5 A g^{-1}	1 M H_2SO_4	S11

Section J. Supporting references

S1 S. Cai, K. Zhang, J. Tan, S. Wang, S. Zheng, J. Fan, Y. Yu, W. Zhang and Y. Liu, *ACS Macro Lett.,* 2016, **5**, 1348-1352.

S2 A. K. M., V. Vijayakumar, S. Karak, S. Kandambeth, M. Bhadra, K. Suresh, N. Acharambath, S. Kurungot and R. Banerjee, *ACS Appl. Mater. Interfaces*, 2018, **10**, 28139-28146.

S3 A. F. M. EL-Mahdy, M. B. Zakaria, H. Wang, T. Chen, Y. Yamauch and S. Kuo, *J. Mater. Chem. A.*, 2020, **8**, 5148-25155.

S4 S. Xiong, J. Liu, Y. Wang, X. Wang, J. Chu, R. Zhang, M. Gong and B. Wu, *J Appl Polym Sci.,* 2022, **139**, 51510.

S5 A. M.t Khattak, Z. A. Ghazi, B. Liang, N. A. Khan, A. Iqbal, L. Li and Z. Tang, *J. Mater. Chem. A.*, 2016, **4**, 16312-16317.

S6 M. Sajjad, R. Tao and L. Qiu, *J Mater Sci: Mater Electron,* 2021, **32,** 1602-1615.

S7 B. Sun, J. Liu, A. Cao, W. Song and D. Wang, *Chem. Commun.*, 2017, **53**, 6303.

S8 M. Ibrahim, H. N. Abdelhamid, A. M. Abuelftooh, S. G. Mohamed, Z. Wen and X. H. Sun, J. Energy Storage, 2022, **55**, 105375.

S9 M. Ibrahim, M. G. Fayed, S. G. Mohamed, Z. Wen, X. H. Sun and H. N. Abdelhamid, ACS Appl. Energy Mater., 2022, **5**, 12828-12836.

S10 P. Bhanja, K. Bhunia, S. K. Das, D. Pradhan, R. Kimura, Yuh Hijikata, S. Irle and A. Bhaumik, *ChemSusChem*, 2017, **10**, 921-929.

S11 S. K. Das, K. Bhunia, A. Mallick, A. Pradhan, D. Pradhan and A. Bhaumik, *Microporous Mesoporous Mater.*, 2018, **266**, 109-116.